Investigation of Joining Performance and Microstructural Mechanisms of Softwood and Hardwood Dowel Joints *via* Rotary Friction Welding

Jian Zhang [a], Yuelong Li [a,*], Hai Zhu,[a] Feng Zhang,[a] Yuchen Zhang,[a] Zhenhe Li,[a] Yanfeng Li,[b] and Yujia Liu [b]

Rotary friction welding of wood typically uses dowels made from the same material as the base wood or involves specific modifications to the dowels, but these methods have practical limitations and are complex. This study focused on commonly used dowel materials (softwood: Scots pine, hardwood: birch), with moisture content adjusted to 7 to 10%, and examined the welding performance and micro-mechanisms. Through orthogonal experiments, the influence of process parameters on the welding strength of both wood types was systematically investigated. The microstructures of the welded areas were analyzed using a depth-of-field microscope and scanning electron microscope (SEM) to explore the friction mechanisms. The results indicated that both Scots pine and birch dowels can be effectively welded using rotary friction. The optimal parameters were identified as follows: Scots pine dowels—hole diameter ratio of 8/12, rotational speed of 3000 r/min, feed rate of 25 mm/s; birch dowels—hole diameter ratio of 8/12, rotational speed of 2500 r/min, feed rate of 20 mm/s. Depth-of-field microscopy revealed larger weld areas and well-preserved surface structures. SEM images showed that during welding, the materials between the dowels and base wood melted, flowed, and re-solidified into a tightly bonded structure, ensuring a durable connection.

DOI: 10.15376/biores.20.3.6267-6285

Keywords: Wood rotary friction welding; Orthogonal experiment; Process parameters; Melting and flow; Welding mechanisms

Contact information: a: College of Mechanical and Electrical Engineering, Northeast Forestry University, No. 26 Hexing Road, Xiangfang District, Harbin, Heilongjiang, China; b: Qiqihar Heping Heavy Ind Grp Co Ltd, Qiqihar 161000, Heilongjiang, Peoples R China;
** Corresponding author: endlesszhang@163.com*

INTRODUCTION

Wood is composed of natural polymers, mainly cellulose, hemicellulose, and lignin. Rotary friction welding of wood dowels involves the generation of heat through friction between a high-speed rotating dowel and a pre-drilled hole in the solid wood, leading to the softening and fusion of lignin and hemicellulose, which form a structure. After cooling, this process results in a high-strength welded interface. Due to its rapid processing, absence of additives and harmful gases, high strength, and high material recovery rate, this technique is considered a green and environmentally friendly method, positioning it as an innovative technology in wood joining. It has made substantial progress, particularly in the development of glue-free bonding in Europe. In comparison with traditional adhesive and metal joining methods, wood welding avoids problems such

as formaldehyde release, poor durability, and metal corrosion, making it widely used in applications such as construction and furniture manufacturing (Zhou *et al.* 2014). In wood rotary friction welding, key factors influencing the welding process include the intrinsic properties of the wood (species, grain direction, *etc*.) and process parameters (dowel rotational speed, feed rate, and the hole diameter ratio between the dowel and the pre-drilled hole in the base material). Additionally, the pre-treatment of both the dowel and the base material significantly affects the welding performance (Luo *et al.* 2017). Current research on the rotary friction welding of wood dowels mainly has explored changes in welding process parameters, physical and chemical transformations during welding, as well as the heat treatment and water resistance of the materials. Budhe *et al.* (2017) demonstrated that at elevated temperatures, resin matrices and adhesives undergo softening, leading to an increase in viscoelastic response. However, the fibers themselves do not degrade. Additionally, temperature fluctuations contribute to progressive debonding and weakening at the material and fiber/matrix interface, primarily due to differences in thermal expansion coefficients between the fibers and resin.

Leban *et al.* (2004) utilized X-ray microdensitometry to examine vibration-welded hardwoods (beech and oak) and softwoods (spruce), revealing a significant increase in wood density at the adhesive interface. The disappearance of intercellular structures at the interface, reduction in voids, and increase in density were positively correlated with bonding strength, with more uniform and pronounced densification yielding stronger joints. Rodriguez *et al.* (2010) investigated the feasibility of high-speed rotary dowel welding in Canadian hardwoods (sugar maple and yellow birch). The study assessed variables such as wood species, grain orientation, rotational speed, and receiving hole diameter. Results indicated that this technique was suitable for both wood types, with average tensile strength comparable to polyvinyl acetate (PVAc) adhesive-bonded joints. Gfeller *et al.* (2004) demonstrated that mechanically induced wood flow welding enables the rapid formation of structurally sound joints without the need for adhesives.

The underlying mechanism primarily involves the melting and flow of amorphous polymers, mainly lignin and partially hemicellulose, facilitating interconnection between wood cells. During welding, long wood cells and fibers partially separate, forming an entangled network within the molten lignin matrix, which subsequently solidifies into a fiber-reinforced composite. Simultaneously, some unbound wood fibers are expelled, while crosslinking reactions occur between lignin and furfural. Zhang *et al.* (2017) welded birch dowels to domestic larch and European spruce substrates, investigating the impact of pre-drilled hole-to-dowel diameter ratios on pull-out resistance and comparing these with direct insertion methods. The study showed that the optimal hole diameter ratio was 9.5/10 for larch substrates and 8.5/10 for spruce substrates. It was emphasized that the pre-drilled hole should be smaller than the dowel to ensure effective friction between the dowel and the wood substrate (Wang and Jin 2019; Zhu *et al.* 2020; He *et al.* 2024). The addition of certain additives or solutions (Pizzi *et al.* 2005; Kubovsky *et al.* 2020) has been shown to improve welding strength within specific ranges. Kubovský *et al.* (2020) found that heat-treated wood exhibited excellent resistance to corrosion, pests, and moisture, enhancing its dimensional and shape stability. Roszyk *et al.* (2020) highlighted the potential of heat-treated wood in construction and humid environments. Li *et al.* (2024) used bamboo dowels instead of wood dowels for rotary friction welding with beech, achieving an adhesive strength of 6.42 MPa, surpassing that of white glue (PVAc).

Scots pine and birch are commonly used wood species in daily life and are high-quality materials frequently utilized in furniture and construction. Heat-treated Scots pine exhibits improved dimensional stability, reducing moisture-induced swelling and shrinkage, and enhancing the wood's resistance to decay and microbial degradation. This treatment significantly boosts the wood's durability and creates a more stable chemical structure, which increases its resilience to environmental factors such as ultraviolet light and precipitation, making it more suitable for outdoor applications. Additionally, the heat treatment deepens the wood's color, giving it a darker brown or reddish-brown hue, which enhances its aesthetic appeal (Zhang *et al.* 2024). In this study, thermally treated Scots pine, a physically modified wood material processed at high temperatures (ranging from 188 to 220 °C) to enhance its properties, was uniformly used as the substrate. Given that the experimental substrate was thermally treated Scots pine, the dowels were also selected from Scots pine to ensure compatibility in terms of thermal expansion coefficient. In contrast, materials such as metal or adhesive have significantly different expansion coefficients from the substrate, which may lead to deformation at the joint due to fluctuations in temperature, humidity, and moisture content, ultimately compromising welding strength. Although using wood with a matching expansion coefficient in the mortise-and-tenon structure can effectively mitigate deformation issues, the machining process is relatively complex and incurs higher manufacturing costs. Furthermore, as Scots pine is a softwood, this study also aims to investigate hardwood (birch wood.) as a dowel material to examine the impact of using materials with different *vs.* identical expansion coefficients on welding strength. Notably, both dowel materials are widely used in the furniture manufacturing industry and are well-accepted in the market. They offer advantages such as affordability, aesthetic appeal, and stable composition, making them highly promising for practical applications. Using orthogonal experiments, the effects of different dowel species on the tensile strength and welding performance of wood rotary welding are investigated. This research aims to provide reference data for optimizing wood welding techniques.

EXPERIMENTAL

Materials

The dowel materials used in this experiment were Scots pine and birch, both of which were smooth dowels with a grain orientation parallel to the wood fibers. The dowels had diameters of 10, 11, 12, and 13 mm, with a uniform length of 100 mm. To facilitate welding, the welding section of each dowel was pre-machined with a chamfer of 8 mm in length at a 45° angle.

The substrate material was thermally treated Scots pine with dimensions of 100 mm × 50 mm × 20 mm (length × width × height). Prior to welding, through-holes with an 8 mm diameter were drilled into the substrate. The moisture content of the dowels was first measured to ensure that it met the target range. If the moisture content deviated from the required range, manual adjustments were made. Ultimately, the moisture content of both the dowels and the substrate was controlled within 7% to 10%. Detailed material parameters are presented in Table 1, while the specific structure of the welded specimens and their through-holes are illustrated in Fig. 1.

Table 1. Specific Parameters of Each Material

	Thermally Treated Scots Pine	Scots Pine Dowel	Birch Dowel
Density (g/cm³)	0.35-0.65	0.39-0.55	0.61-0.72
Compressive Strength Along the Grain (MPa)	58.6	47.4	55
Shear Strength Along the Grain (MPa)	4-8	5	10
Modulus of Elasticity in Bending (GPa)	13	10	12
Hardness (N)	3750	2980	3800
Thermal Conductivity (W/m*K)	0.09-0.13	0.10-0.14	0.12-0.18
Specific Heat Capacity (J/kg*K)	1100-1400	1300-1700	1300-1600

Experimental Procedure

The investigation of wood welding showed that the moisture content of the dowels, rotational speed, feed rate, and hole diameter ratio all significantly affect the strength of wood joints. For this study, dowel diameter, dowel rotational speed, and dowel feed rate were selected as the three primary factors. In order to efficiently handle the multi-factorial experimental design, minimize experimental trials, reduce costs, improve data accuracy and reliability, and facilitate the analysis and application of results, a 3-factor, 4-level orthogonal experimental approach was adopted to evaluate the strength of wood joints under different parameter conditions. The experiment consists of three groups: welding, adhesive bonding, and impact testing, for comparative analysis.

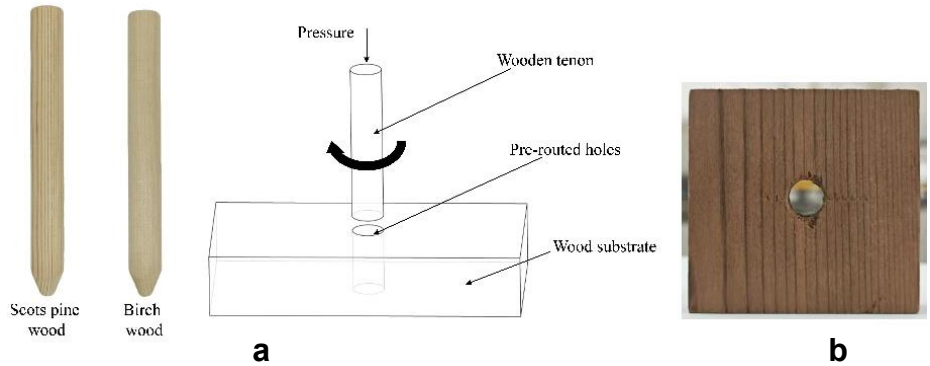

Fig. 1. Schematic diagram of welded specimen and its through-hole structure

In the welding group, dowels with varying diameters were inserted into 8 mm pre-drilled holes through high-speed rotation, with a welding depth of 22 mm. In the adhesive bonding group, dowels with a diameter of 7.8 mm were lathed and inserted into the 8 mm pre-drilled hole. The gap fit ensures that the hole diameter exceeds the dowel diameter, creating space for polyvinyl acetate (PVAc) adhesive to be evenly spread on the dowel surface, preventing excessive adhesive overflow during insertion into the substrate. The adhesive bonding depth was the same as the welding depth. In the impact testing group, a

10 mm dowel was hammered into the 8 mm pre-drilled hole using a wooden mallet, with a depth of 22 mm. Each test group consists of three sample sets, and the average values were analyzed.

The orthogonal experimental design and the corresponding data are presented in Table 2.

Table 2. Factor Levels for the Orthogonal Experiment

Group	Factor	Levels			
		1	2	3	4
A	Dowel/Hole Ratio	10/8	11/8	12/8	13/8
B	Rotational Speed (r/min)	2500	3000	3500	4000
C	Feed Rate (mm/s)	10	15	20	25

Experimental Equipment for Wood Rotational Welding

The welding experimental setup and test platform are shown in Fig. 2. Prior to use, the substrate must be securely fixed to the experimental platform with a bench clamp, and holes should be pre-drilled in the substrate. The surface of the substrate and the pre-drilled holes should be carefully cleaned to remove wood dust, ensuring high-quality welding. For better welding results, the dowel is clamped firmly, and the spindle drives the dowel to rotate at high speeds. The rotational speed of the dowel and the feed rate are adjustable *via* the control panel. When the high-speed rotating dowel comes into contact with the substrate, friction generates heat, causing lignin and other components to melt. After the temperature drops, the welding zone solidifies, completing the welding process.

a b

Fig. 2. Wood welding equipment

The mechanical performance of the specimens was evaluated following the GB/T 14018 (2009) standard. The study measures the pull-out strength of the dowel joints, using a WDW100 universal testing machine. The specimen is mounted using special clamps, with the upper clamp holding a length of approximately 40 mm, while the lower substrate is firmly positioned against the clamp surface (Fig. 3). The stretching speed is 5 mm/min until the dowel is completely pulled out.

After welding, samples measuring 20 mm × 20 mm × 2 mm (length × width × height) are taken for microscopic examination. The microstructure of the welded zone and surface is analyzed using a Keyence VHX-2000 super-depth three-dimensional microscope (Fig. 4a).

To observe the structural changes at the welded joint and interface, samples measuring 10 mm × 10 mm × 5 mm (length × width × height) were selected for further analysis. After cleaning the surface dust, the samples were gold-coated in a sputtering chamber. A COXEM EM-30N scanning electron microscope was then used to observe the microscopic features of the welded joint and interface, analyzing structural changes before and after welding to better understand the welding mechanism (Fig. 4b).

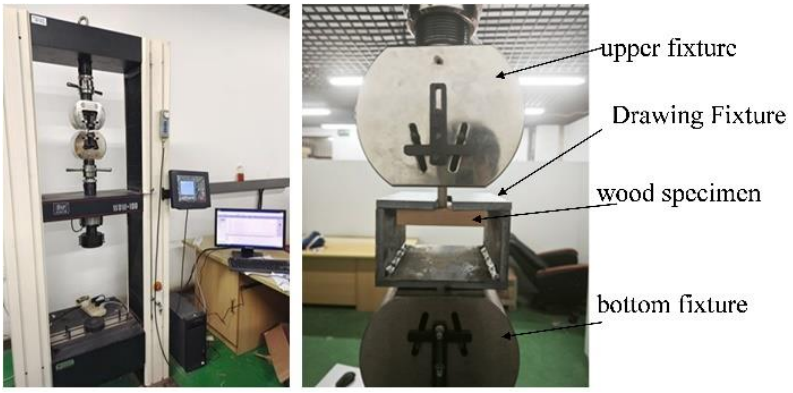

Fig. 3. Wood tensile testing equipment

Fig. 4. a: Super depth-of-field equipment and b: scanning electron microscopy

RESULTS AND DISCUSSION

Analysis of Dowel Material on Welding Strength

Wood species are crucial determinants of welding strength. Due to their varying structures, chemical compositions, and densities, different species of wood display distinct physical and chemical responses during welding, which can significantly affect the strength of the weld. Coniferous and broadleaf species show marked differences in cell wall thickness, lumen size, and fiber structure, which directly influence the quality of the welded joint. For example, coniferous species such as Scots pine, characterized by a pronounced difference between earlywood and latewood, tend to produce more uniform weld zones, enhancing welding performance. In contrast, broadleaf species such as oak, with denser fiber cells, are more prone to localized charring during welding, leading to compromised weld quality.

The density of wood species plays a crucial role in heat conduction and the compactness of the welded joint during the welding process. High-density woods, such as oak, accumulate heat more rapidly during welding, leading to greater compression of the weld zone, which facilitates the formation of a stronger bond. In contrast, low-density woods, such as poplar, have higher porosity and lower thermal conductivity, resulting in uneven heat distribution in the weld region. This may lead to insufficient melting or incomplete bonding, ultimately reducing the welding strength (Yu *et al.* 2011).

Additionally, the relative proportions of lignin, hemicellulose, and cellulose in wood significantly affect the melting, softening, and chemical bonding processes during welding. Woods with higher lignin and hemicellulose content are more likely to produce stable, fused weld zones, thus achieving higher welding strengths (Gedara *et al.* 2021). For instance, Scots pine, which contains a relatively high level of lignin, exhibits stronger bonding after welding, while broadleaf species like poplar, with lower hemicellulose content, typically show weaker welds.

This study investigated the impact of two different wood species, Scots pine and birch, on welding strength by conducting orthogonal experiments on two types of dowels. The results of the orthogonal experiments are as follows (kx and kxx represent Scots pine and birch, respectively).

Table 3. Orthogonal Experiment Design and Experimental Results

Experiment No.	Factors Affecting			Average Tensile Strength (N)	
	A	B	C	Birch wood	Scots pine wood
1	1	1	1	130.5	232.5
2	1	2	2	183.5	431.5
3	1	3	3	205	108.5
4	1	4	4	155	384.5
5	2	1	2	765	435.25
6	2	2	1	265	589
7	2	3	4	874.25	500.5
8	2	4	3	942.25	439.5
9	3	1	3	1637.5	612
10	3	2	4	1239.25	1427.75
11	3	3	1	297.25	611.75
12	3	4	2	643.25	546.25
13	4	1	4	1174.25	833
14	4	2	3	1144.75	761.25
15	4	3	2	413.5	980
16	4	4	1	303.75	246.5
Mean (k_1)	168.5	926.81	249.13		
(k_{11})	289.25	528.19	419.94		
Mean (k_2)	711.69	708.13	501.31		
(k_{22})	491.06	802.38	598.25		
Mean (k_3)	954.31	447.5	982.38		
(k_{33})	799.31	550.19	480.31		
Mean (k_4)	759.06	511.06	860.69		
(k_{44})	705.19	404.19	786.44		
extreme deviation 1	785.81	479.31	733.25		
extreme deviation 2	510.06	398.19	366.5		

By analyzing the orthogonal experiment results for the two materials, the factors influencing tensile strength were found to differ in their significance. For birch, the order of influence was aperture ratio > rotation speed > feed rate. For Scots pine, the sequence was aperture ratio > feed rate > rotation speed.

The average tensile force, shown in Fig. 5, indicated that the optimal aperture ratio for both materials was 8/10. When the aperture ratio exceeded 8/10, the average tensile force decreased. The tensile force for birch decreased as rotation speed increased. In contrast, for Scots pine, tensile force increased initially and then decreased as the rotation speed increased. The feed rate had a similar trend, first increasing and then decreasing the tensile force, with a greater influence on birch compared to Scots pine.

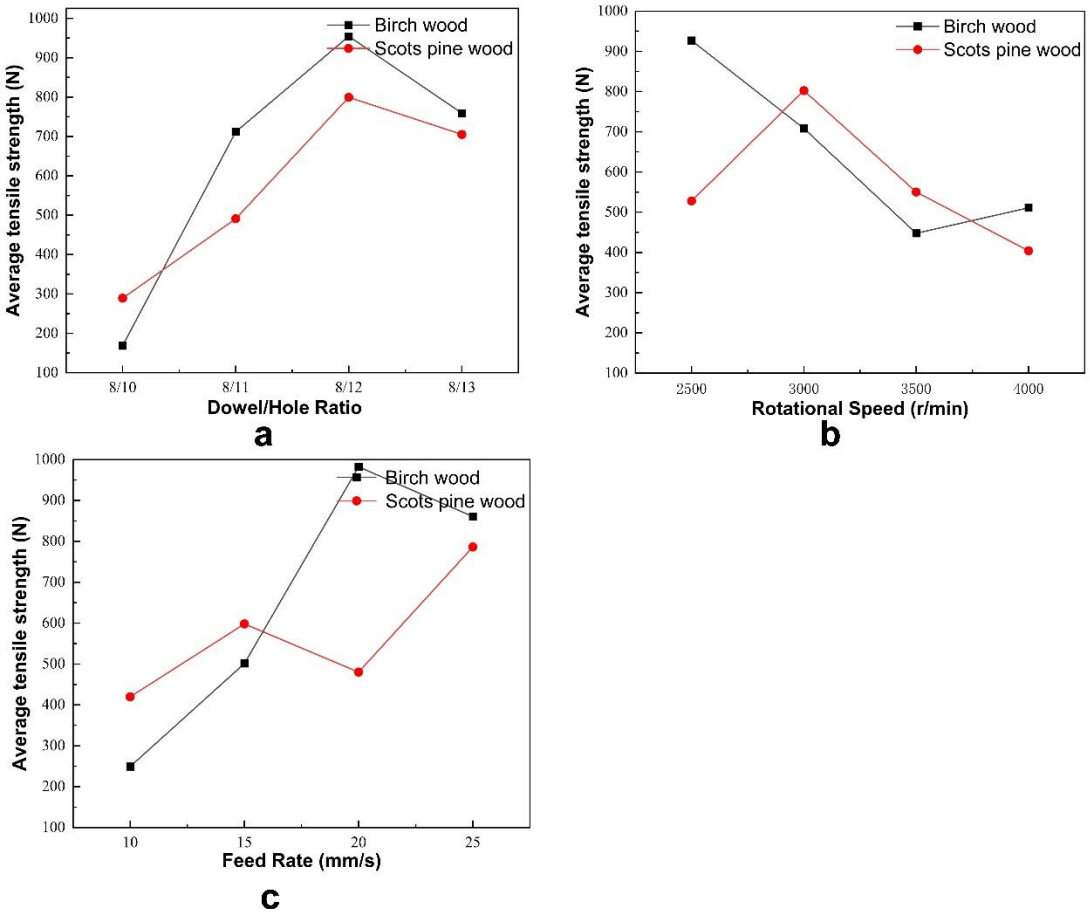

Fig. 5. Average pull-out force chart

Comparative Analysis of Connection Strengths for Different Joining Methods (Welding, Adhesive Bonding, and Hammering)

Under specific testing conditions, experiments were conducted for both the adhesive bonding and hammering groups, and the tensile forces were measured. The results were then compared with the welding strength achieved under optimal welding parameters. The dowel diameter for the test specimens was 10 mm, with an 8 mm diameter for the pre-drilled holes. To ensure uniformity in the weld zone, the welding, hammering, and adhesive bonding depths were all set to 22 mm, and the insertion depth of the dowels was also 22 mm. The results of the experiments are presented in Table 4. The connection strength in the welding group was significantly higher than in both the adhesive bonding and

hammering groups. This indicates that rotational friction welding offers a significant advantage in enhancing the connection strength between two different dowel types, further confirming the effectiveness and practicality of wood friction welding technology.

Table 4. Comparison of Connection Strengths for Hammering, Adhesive Bonding, and Welding Groups

Experimental Group	Average (N)		Coefficient of Variation		Maximum (N)		Minimum (N)	
	Scots Pine	Birch	Scots Pine	Birch	Scots Pine	Birch	Scots Pine	Birch
Welding Group	1427.75	1637.5	5.24%	1.17%	1519.0	1658.5	1336.0	1616.50
Adhesive Bonding Group	1116.17	1018.33	14.31%	17.36%	1323.0	1265.0	934.0	860.0
Hammering Group	382.67	391.67	7.80%	8.90%	415.0	439.0	343.0	356.0

Tensile tests were performed on the welding, adhesive bonding, and hammering specimens, and typical force-displacement curves were generated. Figure 6 shows the curves for the best specimens in each group.

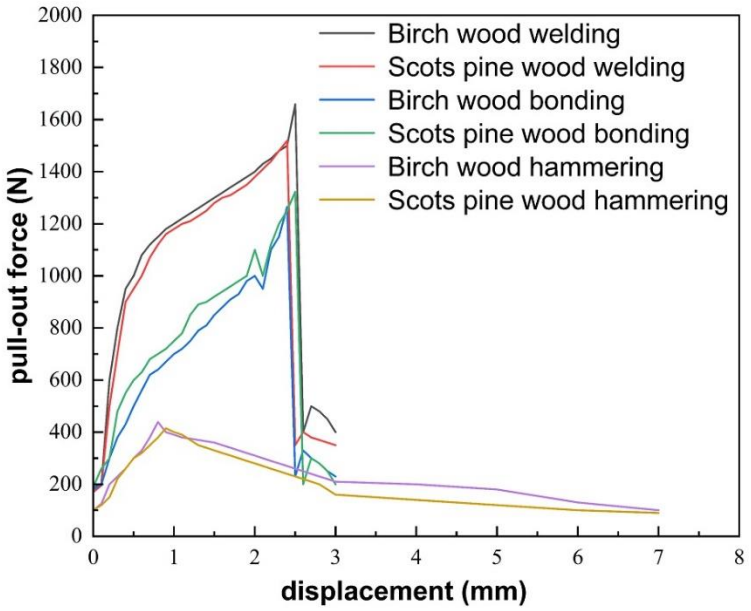

Fig. 6. Pull-out force-displacement curves for each group

At the initial stage, the curves for specimens within the same group coincided, which is attributed to the pre-tightening process of the fixture. Once pre-tightening was complete, the tensile curves for the welding and adhesive bonding groups began to show clear differences from those of the hammering and base material groups. The curves can be divided into three distinct stages: the elastic stage, the yielding stage, and the extension failure stage. The changes in the welding and adhesive bonding groups were more noticeable, while the curve for the hammering group exhibited a more gradual change. The strength in the hammering specimens mainly resulted from the mechanical interlocking of

rough peaks on the wood surface, combined with elastic-plastic deformation and static friction at the microscopic level. This generates lower connection strength, quickly reaching the maximum tensile force, after which the dowel is pulled out. In contrast, the welding and adhesive bonding specimens experienced a sharp decline in force after reaching the maximum tensile force, due to failure at the joint interface. Although friction was still present, the force decreased to a certain level and then stabilized. As the dowel was extracted or damaged, the pull-out force gradually diminished and became stable.

Macro-Morphological Analysis of Wooden Dowel

Birch is a widely distributed broadleaf species that is known for its light and soft texture, with straight grain that makes it easy to work with. The macroscopic structure of birch is typically smooth, without any significant or distinctive textures or features. Scots pine, a coniferous species found mainly in northeastern China, is light in weight but possesses good durability, strong resistance to deformation, and a certain level of bending, compressive, and impact strength. The wood of Scots pine is light-colored, aesthetically attractive, and easy to paint or dye.

In this study, a round dowel rotational wood welding technique was employed, where birch and Scots pine dowels were inserted into pre-drilled round holes. During high-speed rotation, friction between the dowel and the hole wall generates heat, causing the wood fibers to soften and melt, eventually forming a welding zone that connects the two materials. After welding, the dowels were pulled from the welded region to observe their macroscopic morphology. The welded materials and the morphology after dowel extraction in the orthogonal experimental group are shown in Fig. 7. A black layer, corresponding to the welding interface, is visible on the surface of the extracted dowel. It can be seen that the welded surface of the birch dowel exhibits better uniformity than that of the Scots pine dowel.

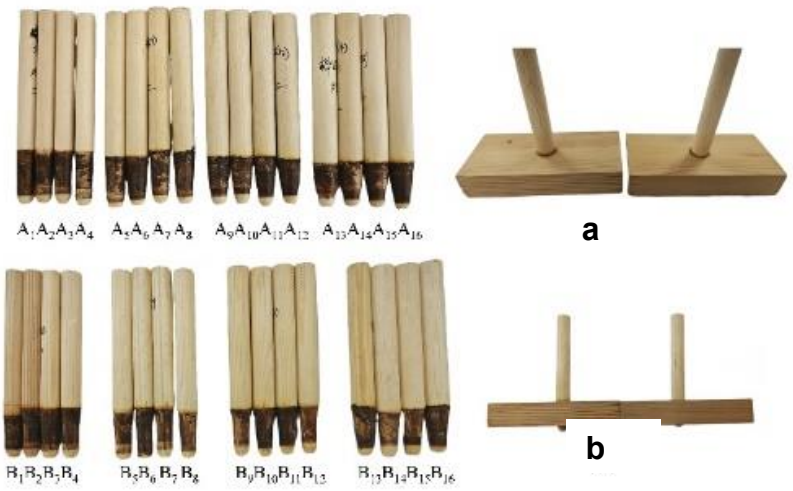

Fig. 7. Macroscopic morphology of wood dowel welded joints. A1-A16 show the images of birch dowels from the orthogonal experiment, while B1-B16 depict the images of Scots pine dowels from the orthogonal experiment.(a) and (b) represent the specimens after wood welding.

In the wood rotational welding process, a certain amount of white smoke and wood chips are produced, as illustrated in Fig. 8 (a, c represent birch, b, d represent Scots pine). The generation of white smoke is a common occurrence during wood rotational welding, primarily due to the pyrolysis of the wood and the release of volatile substances at high temperatures. The amount and composition of white smoke differ depending on the type

of dowel material. Scots pine, as a conifer, is rich in resin and terpenic compounds. During rotational welding, the interface temperature rapidly increases (typically between 200 and 300 °C), causing the resin and terpenes to volatilize. The high temperature also leads to the dehydration and degradation of hemicellulose in Scots pine, producing small volatile molecules such as furfural. Partial pyrolysis of lignin releases phenolic and aromatic compounds, which break down and release gases, becoming the primary sources of white smoke. Birch, as a broadleaf species, contains less resin but is abundant in polysaccharides and lignin. Under high temperatures, the pyrolytic volatiles from birch mainly consist of furfural, acetic acid, and phenolic substances. Due to the differing chemical compositions of Scots pine and birch, their volatile compounds differ in type and quantity, resulting in slight variations in the color and intensity of the white smoke. For instance, Scots pine, with its higher resin content, produces a greater volume of white smoke with a distinct wood scent, due to the contributions of terpenes and resins. Birch, with its lower resin content, produces less white smoke, which is primarily composed of polysaccharide degradation products (such as acetic acid and furfural) and lignin pyrolysis products, leading to a lower smoke volume but a more acidic smell.

The generation of wood chips occurs due to the intense friction between the dowel and the base material, caused by the high rotational speed and pressure. This phenomenon is influenced by the dowel species and its pyrolytic characteristics. In Scots pine, lignin softens and flows at high temperatures, and part of it combines with hemicellulose degradation products to form the molten zone. The high temperature causes the resin in the dowel to melt and seep out, bonding with the wood chips to form a finer and denser layer of wood dust, some of which infiltrates the welding zone, reducing the amount of wood dust generated on the base material's surface. Birch, being harder than Scots pine, generates more shear force during rotational welding, causing the wood fibers on the base material surface to break. The pyrolysis degree of birch is lower than that of Scots pine, and without the adhesive effect of resin, the wood dust is looser and tends to accumulate around the welding zone, resulting in more wood dust production.

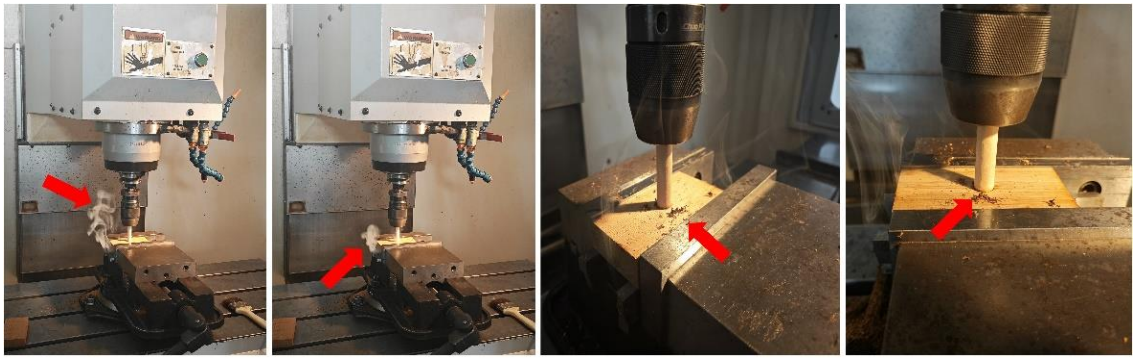

a b c d

Fig. 8. Smoke produced during the welding of (a) birch and (b) Scots pine, with arrows indicating the areas where smoke was generated during the welding process. Sawdust produced during the welding of (c) birch and (d) Scots pine, with arrows pointing to the areas where sawdust was generated.

Observation and Analysis Using an Extended Depth of Field Microscope System

Figure 9 presents the results of super-depth microscopy of the welding interface of Chinese pine, comparing the regions welded under optimal parameters (10) (a, c) and those welded under suboptimal parameters (1) (b, d). Panels (a) and (b) show planar views, while panels (c) and (d) depict the corresponding three-dimensional morphological maps. In Fig. 9(a), the region with better welding quality exhibits a uniform, dense interlaced fiber structure, with fibers at the welding interface tightly bonded, indicating that the wood in this region has undergone sufficient softening and flow. The corresponding three-dimensional morphology (Fig. 9c) further reveals lower surface roughness and a uniform height distribution, with a small height difference between the highest and lowest points (approximately 400 μm).

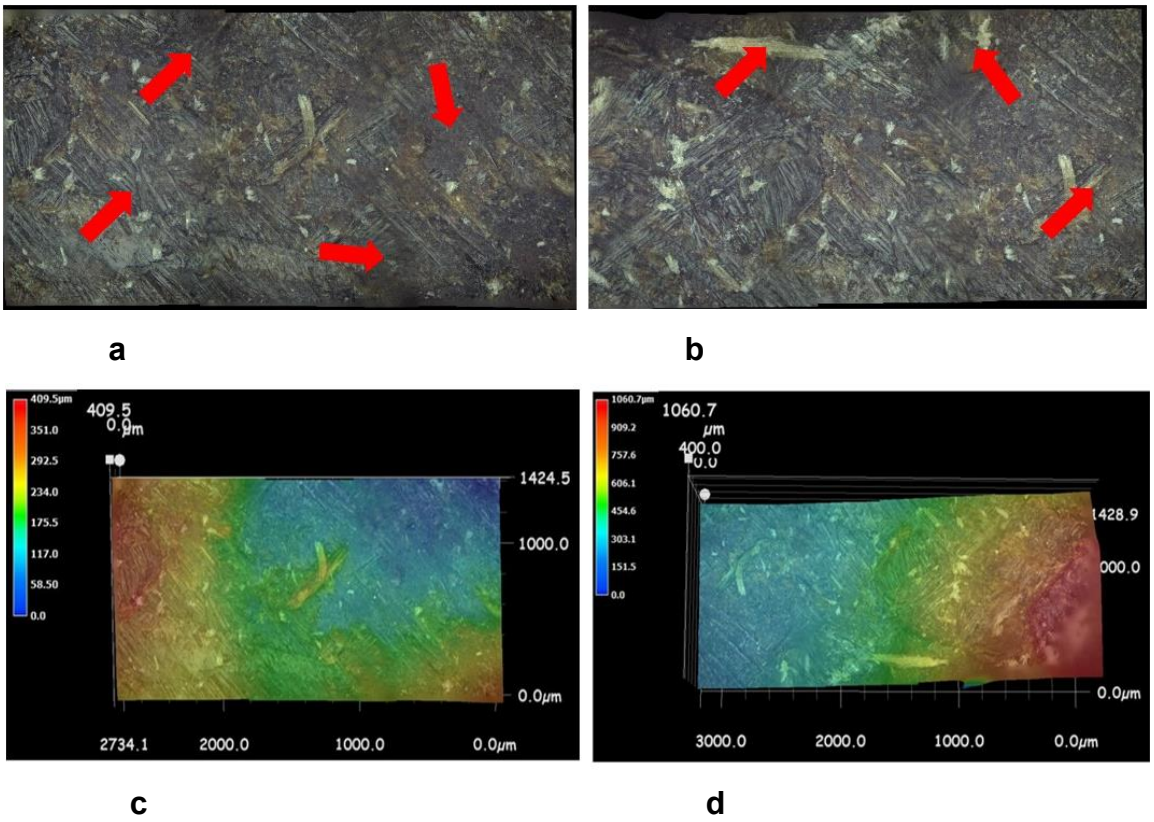

Fig. 9. Super-depth microscopic images of Scots pine. (a) 2D super-depth image of the welding joint under optimal parameters, with arrows marking the areas with good weld quality; (b) 2D super-depth image of the welding joint under poor parameters, where the arrows point to the suboptimal welding zones; (c) 3D super-depth image showing the results under the best parameters; and (d) 3D super-depth image under less favorable welding conditions

Figure 10 presents the super-depth microscopy results of the welding interface of birch, comparing the regions welded under optimal parameters (9) (e, g) and those welded under suboptimal parameters (1) (f, h). Figures (e) and (f) show planar images, while figures (g) and (h) display the corresponding three-dimensional morphological maps.

As shown in Fig. 10e, the region with better welding quality exhibited a smooth and uniform interface with tightly bonded fibers, indicating that the thermal softening and material flow of the wood in this region were adequately achieved during welding. The

corresponding three-dimensional morphology (Fig. 10g) shows a small height difference (approximately 562 μm), suggesting low surface roughness and good flatness of the welding interface.

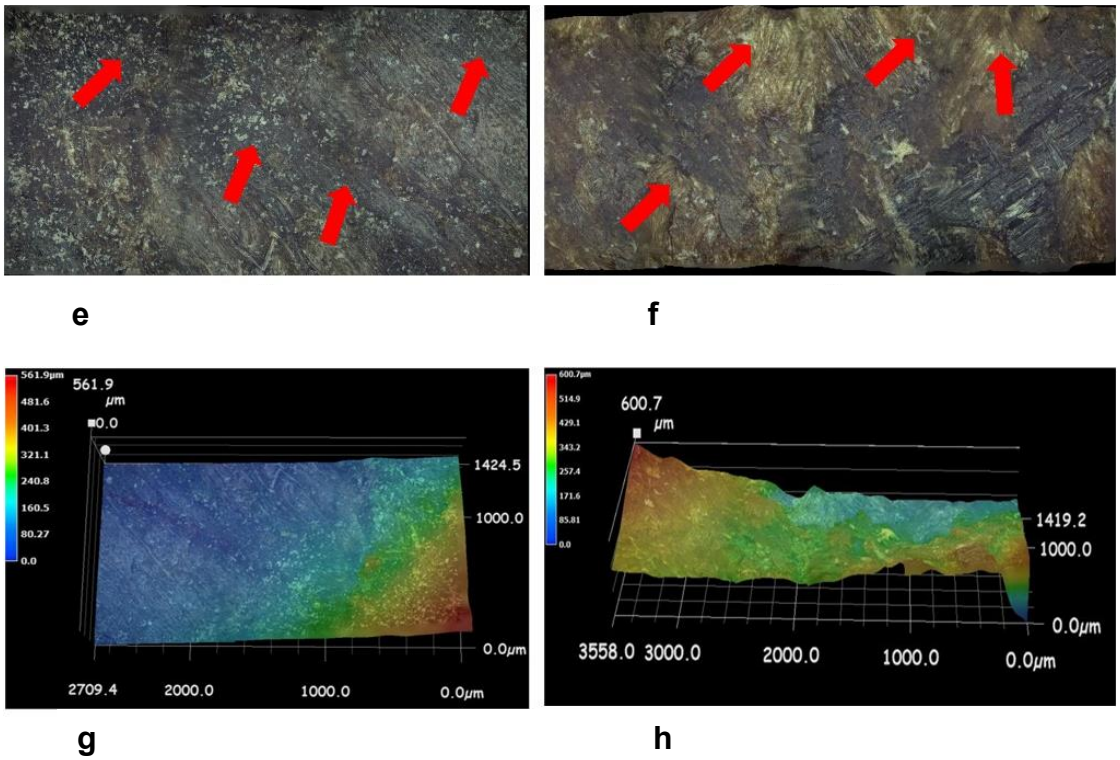

Fig. 10. Super-depth Images of birch wood. (e) A super-depth 2D image of the welded joint under optimal parameters, with arrows indicating areas of good welding zones; (f) a super-depth 2D image of the welded joint under suboptimal parameters, with arrows pointing to areas of poor welding zone; (g) a super-depth 3D image under the best parameters; and (h) a super-depth 3D image under the less favorable parameters

In contrast, the region with poorer welding quality in Fig. 10f exhibits a rougher interface with loose fiber bonding and noticeable fiber stretching and separation. The three-dimensional morphology (Fig. 10 h) further reveals a significant increase in height difference, reaching approximately 601 μm, with greater and uneven surface fluctuations. This interface defect is likely due to uneven heat or pressure distribution during welding, resulting in insufficient softening and flow of the wood fibers.

The results show that the microscopic morphology of the welding interface impacted the welding quality. The region with better welding quality featured a more uniform interface and denser fiber bonding, whereas the region with poor welding quality exhibits significant interface defects due to incomplete softening, which may be closely related to mismatched welding parameters (such as temperature, pressure, and time).

A comparison of the super-depth microscopy results between Chinese pine (a-d) and birch (e-h) welding interfaces shows that the left side of both wood types corresponds to the regions with better welding quality (a, c, e, g), while the right side corresponds to the regions with poorer welding quality (b, d, f, h). The planar images and three-dimensional morphology maps were analyzed to explore the microscopic features of the welding interfaces in both wood types. In the regions with better welding quality (a, c, e, g), both Chinese pine and birch exhibited dense fiber bonding at the welding interface, but

their morphological characteristics differed. The Chinese pine interface (a, c) displayed a more uniform fiber arrangement, and the three-dimensional morphology showed a smaller surface height difference (approximately 400 μm), indicating better interface flatness. In contrast, the birch interface (e, g), while tightly bonded, showed a more random fiber arrangement, and the height difference in the three-dimensional morphology was slightly larger (approximately 562 μm). This difference may arise from the structural and thermal softening characteristics of the two wood types, with Chinese pine having longer fibers and a more uniform cellular structure, which facilitates the formation of a smoother interface during welding.

In the regions with poorer welding quality (b, d, f, h), both wood types exhibited poor fiber bonding and a significant increase in surface roughness. The Chinese pine interface (b, d) showed noticeable fiber separation and cracks, with the height difference increasing to 1060 μm, reflecting substantial surface fluctuations. The birch interface (f, h) showed more irregular fiber breakage and separation, with a height difference of 601 μm. Although the surface fluctuation was smaller than that of Chinese pine, the interface unevenness was more pronounced. This suggests that the thermal softening and flow properties of birch during welding may be weaker than those of Chinese pine, leading to more interface defects.

In conclusion, significant differences exist between Chinese pine and birch in terms of welding interface morphology and bonding quality. The Chinese pine welding interface is more likely to form a smooth and dense bond, and it showed higher adaptability to welding process parameters (such as temperature and pressure). In contrast, the birch interface was more susceptible to uneven thermal softening, and its welding quality was more sensitive to process parameters. Therefore, it is essential to optimize the welding process parameters according to the characteristics of different wood types to improve welding quality.

Analysis of Scanning Electron Microscope (SEM) Results

Samples of the wooden dowel rod were taken from the front end after welding and observed under a scanning electron microscope (SEM). The dimensions of the samples from both materials were 10 mm × 10 mm × 5 mm, as shown in Fig. 11.

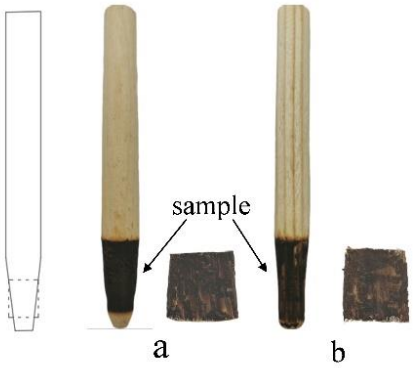

Fig. 11. Sample pieces taken from the welded dowel of (a) birch and (b) Scots pine

Through SEM analysis, the interlocking structure of the welding zone could be observed. Under the condition of 10.0, the molten wood components after welding were clearly seen to re-aggregate and interlock, forming the welding interface and tightly

connecting the wooden tenon with the base material, thereby providing mechanical strength to the weld joint. SEM images of the tenons made from two different materials are shown in Fig. 12, with (a) showing the scanning electron microscope image of pine and (b) showing that of birch. The welding zone is indicated by arrows, and the quality of the welding zone can be clearly seen. These observations confirm that the softening and flow of the wood cells during welding resulted in the formation of a tightly interwoven structure after cooling.

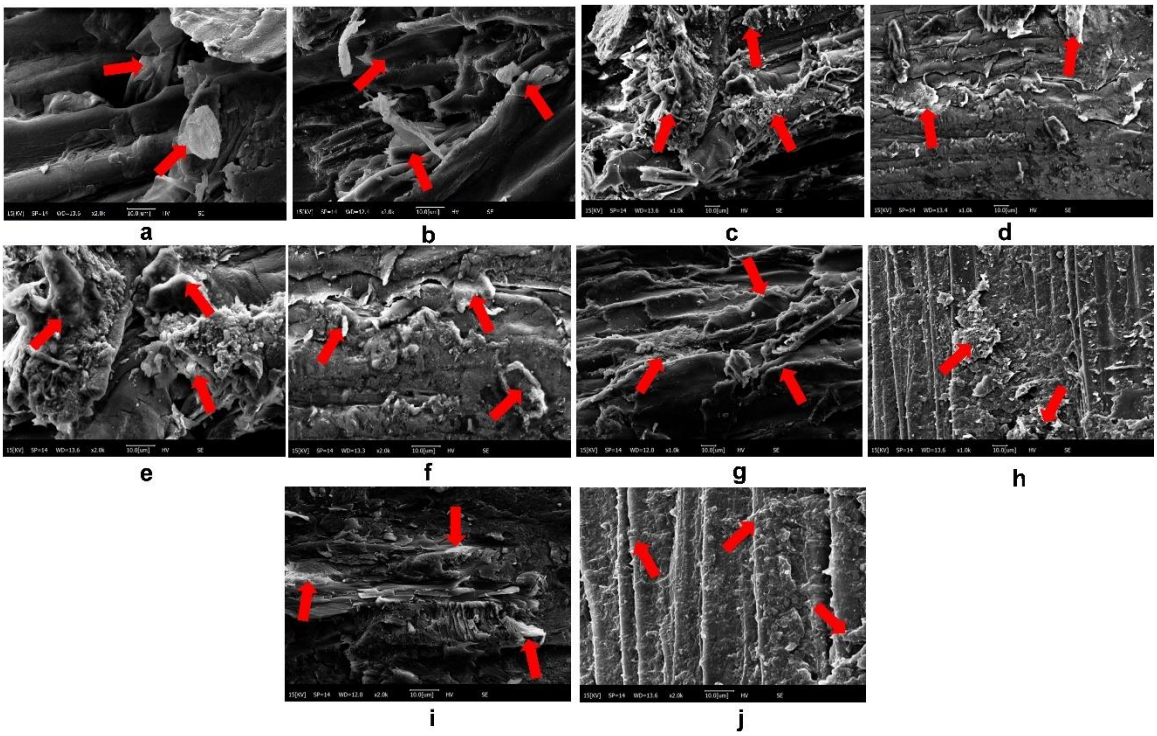

Fig. 12. Microstructure of the wood after welding

Figures 12c, d, e, and f show the scanning electron microscope (SEM) images of the welding zones of Scots pine wood after welding. Figures 12c and d represent the surface morphology of the tenon sample taken from the head of the Scots pine tenon, with (c) showing the condition of better welding (numbered 10) and (d) showing the condition of poorer welding (numbered 1). A comparison reveals that, under the better welding condition, lignin, hemicellulose, and other components were fully melted and flowed, resulting in a well-formed welding zone that leads to a higher welding strength of the wood. Under the poorer welding condition, although there is some flow of lignin, hemicellulose, and other components, the melting and flow are insufficient, and the welding zone formed on the surface is noticeably poor, leading to lower welding strength.

Figures 12c and e show the welding surface morphology of the better quality tenon sample from the head of the tenon. Figures 12c and d were observed at 1000x magnification, and Figs. 12e and f were observed at 2000x magnification. It is evident that the fibers on the substrate hole wall and the fibers on the tenon surface had become welded together, with the fibers arranged nearly perpendicular to each other, forming a dense and thick welding zone. In contrast, figures d and f display the morphology of the welding zone in the poorer quality case, showing that the fibers on the substrate hole wall and the fibers on the tenon surface are not adequately welded together, with some areas showing no

welding zone at all.

Figures 12g, h, i, and j depict the SEM images of birch wood tenons. Figure 12g shows the better welding condition (numbered 9), while figure h shows the poorer welding condition (numbered 1). Figures 12g and i display the SEM images of the birch tenon's welding interface at different magnifications. Figure 12g, at 1000x magnification, shows a uniform and continuous molten state of the fibers in the welding zone, with tightly bonded fibers and minimal molten material on the surface, reflecting better welding quality. Figure 12i, observed at 2000x magnification, provides a clearer view of the micro-adhesion between the fibers at the welding interface, further confirming the high-quality bonding characteristics.

In contrast, Figs. 12h and j show the interface morphology of birch wood when the welding quality was poor. At 1000x magnification (Fig. 12h), the fibers are loosely arranged, and there was noticeable delamination in the welding zone, with many fragments and incompletely melted fiber pieces. At 2000x magnification (Fig. 12j), the welding zone fibers have not effectively bonded, and the surface was rough, exhibiting micro-cracks and residual material, indicating poor welding quality.

The bonding mechanism of binderless boards has attracted considerable research attention and has been extensively studied (Zhang *et al.* 2015; Tajuddin *et al.* 2016; Hubbe *et al.* 2018;). During heat treatment or hot pressing, hygroscopic hemicellulose undergoes degradation, producing soluble sugars. These sugars further react, reducing their hygroscopicity and forming highly branched polysaccharides. Additionally, the free sugars derived from hemicellulose degradation can polymerize during hot pressing, effectively acting as natural adhesives. Furthermore, the thermal softening of lignin allows the cell wall matrix to reorganize upon compression, forming a new structure with reduced internal stress. Ultimately, crosslinking occurs between lignin and carbohydrate polymers, as well as among carbohydrate polymers themselves, enhancing material stability and bonding performance.

The welded areas observed on the surfaces of the two types of wood also showed some differences at the same magnification. A certain degree of speculation through existing studies by others suggests that the possible reason for this effect is the difference in cell structure and chemical composition.

Cellular structure differences

Softwoods and hardwoods have significant differences in their cell types and arrangement patterns. Hardwoods typically contain vessel elements, rays, and fibers, while these structures are less common in softwoods. The vessels and fibers in hardwoods provide higher strength and density, whereas softwoods are mainly composed of tracheids, which have lower density. These structural differences in cells result in distinct micro-morphologies during the welding process.

Chemical composition differences

Hardwoods have a higher content of hemicellulose (such as xylan) and lignin, which are more easily melted and flowed during welding, forming a dense interface layer. In contrast, softwoods mainly consist of glucan, which has a lower melting point. During welding, glucan tends to volatilize and decompose more easily, leading to a rougher welding interface. Microstructural Characteristics of the Welding Interface: During welding, the interface layer of hardwoods is typically more uniform and dense, while softwoods' interface layers may appear uneven due to the volatilization and decomposition

of their chemical components. Additionally, the higher elastic modulus of hardwoods gives them higher bonding strength after welding, whereas softwoods, with their lower density and strength, tend to have lower bonding strength post-welding.

Both Scots pine and birch are commonly used woods. However, due to differences in wood density, they can be categorized into softwoods and hardwoods. The primary differences in their welding surfaces during the welding process are attributed to variations in their cellular structures, chemical compositions, and the microstructural characteristics of the welding interfaces. These differences determine the welding performance and the final characteristics of the welded surfaces.

Future research may further explore the effects of process parameters on welding temperature, and the mechanisms of wood component degradation and re-polymerization under high temperatures to gain a deeper understanding of the mechanism behind rotary friction welding of wood.

CONCLUSIONS

1. Experimental results indicated that wood rotary friction welding is an efficient and viable joining technique. Under optimal process parameters, the welding strength is significantly superior to traditional methods such as impact and adhesive bonding, confirming the effectiveness of this technology. This study determined the optimal process parameters for two types of wood: for Scots pine, the best parameters were a rotational speed of 3000 r/min, a feed rate of 25 mm/s, and a hole diameter ratio of 8/12; for birch, the optimal parameters were a rotational speed of 2500 r/min, a feed rate of 20 mm/s, and a hole diameter ratio of 8/12.
2. Further analysis of the influence of process parameters on welding strength revealed the following order of significance: for birch, the welding strength was primarily influenced by the hole diameter ratio, followed by rotational speed, and lastly, the feed rate. In contrast, for Scots pine, the order of influence was hole diameter ratio, feed rate, and rotational speed. When the hole diameter ratio exceeded 8/10, the average pull-out force of both wood types decreased. The pull-out strength of birch gradually decreased with increasing rotational speed, while Scots pine's pull-out strength increased initially before decreasing. The feed rate showed a trend of first increasing and then decreasing the pull-out force, with birch being more sensitive to changes in feed rate.
3. The study also found that dowel material has a significant effect on welding strength. Under the optimal welding parameters, birch dowels exhibit higher welding strength than Scots pine dowels, likely due to birch's higher density and tightly packed fiber structure, which facilitates heat transfer and the formation of a uniform welding zone. Furthermore, the decomposition products released by birch at high temperatures may enhance the interface bonding.
4. Three-dimensional super-depth observations revealed height differences in the welding surfaces of both wood types, indicating that process parameters affected the uniformity of the welding zone surface. Scots pine welding interfaces tended to form flat and dense bonded regions more easily, whereas birch was more susceptible to uneven thermal softening, making its welding quality more sensitive to process parameters.
5. Scanning electron microscopy showed that in the course of welding, the wood

components melted and re-solidified, thereby forming a tightly interwoven structure that firmly connects the dowel and substrate. The welding zone analysis showed that the fibers on the substrate hole walls and dowel surface interlock, with traces of wood component flow observed in some regions. This phenomenon reveals the basic mechanism of rotary friction welding of wood: the high-speed rotation of the dowel generates heat through friction with the substrate, causing the components between wood cells to melt and flow. After welding stops, these molten components solidify quickly, resulting in a strong connection.

REFERENCES CITED

Budhe, S., Banea, M. D., de Barros, S., and daSilva, L. F. M. (2017). "An updated review of adhesively bonded joints in composite materials," *International Journal of Adhesion and Adhesives* 72, 30-42. DOI: 10.1016/j.ijadhadh.2016.10.010

GB/T 14018 (2009). "Wood nail withdrawal testing," Standardization Administration of China, Beijing.

Gedara, A. K., Chianella, I., Endrino, J. L., and Zhang, Q. (2021). "Adhesiveless bonding of wood – A review with a focus on wood welding," *BioResources* 16(3), 6448-6470. DOI: 10.15376/biores.16.3.Gedara

Gfeller, B., Pizzi, A., Zanetti, M., Properzi, F., Lehmann, M., and Delmotte, L. (2004). "Solid wood joints by *in situ* welding of structural wood constituents," *Holzforschung* 58(1), 45-52. DOI: 10.1515/hf.2004.007

He, J. R., Wu, J. W., and Yang, Y. (2024). "Research progress on the rotary friction welding technology," *China Forest Products Industry* 61, 32-38. DOI: 10.19531/j.issn1001-5299.202408007

Hubbe, M. A., Pizzi, A., Zhang, H. Y., and Halis, R. (2018). "Critical links governing performance of self-binding and natural binders for hot-pressed reconstituted lignocellulosic board without added formaldehyde: A review," *BioResources* 13(1), 2049-2115. DOI: 10.15376/biores.13.1.Hubbe

Kubovsky, I., Kacíková, D., and Kacík, F. (2020). "Structural changes of oak wood main components caused by thermal modification," *Polymers* 12(2), 485. DOI: 10.3390/polym12020485

Leban, J. M., Pizzi, A., Wieland, S., *et al.* (2004). "X-ray microdensitometry analysis of vibration-welded wood," *Journal of Adhesion Science and Technology* 18(6), 673-685. DOI: 10.1163/156856104839310

Li, S., Zhang, H., and Cheng, L. (2021). "Bonding properties of bamboo dowel (nail) welded to wood with high speed rotation," *J. Northwest For. Univ* 36, 225-232. DOI: 10.3969/j.issn.1001-7461.2021.04.33

Luo, X., Zhu, X., and Zhang, J. (2017). "Theoretical research and technical progress of wood welding," *Journal of Northwest Forestry University* 32(6), article 270. DOI: 10.3969/j.issn.1001-7461.2017.06.43

Pizzi, A., Leban, J. M., Zanetti, M., Pichelin, F., Wieland, S., and Properzi, M. (2005). "Surface finishes by mechanically induced wood surface fusion," *Holz Als Roh-Und Werkstoff* 63(4), 251-255. DOI: 10.1007/s00107-004-0569-8

Roszyk, E., Stachowska, E., Majka, J., Mania, P., and Broda, M. (2020). "Moisture-dependent strength properties of thermally-modified *Fraxinus excelsior* wood in compression," *Materials* 13(7), article 1647. DOI: 10.3390/ma13071647

Rodriguez, G., Diouf, P., Blanchet, P., and Stevanovic, T. (2010). "Wood-dowel bonding by high-speed rotation welding - Application to two Canadian hardwood species," *Journal of Adhesion Science and Technology* 24(8-10), 1423-1436. DOI: 10.1163/016942410x501025

Tajuddin, M., Ahmad, Z., and Ismail, H. (2016). "A review of natural fibers and processing operations for the production of binderless boards," *BioResources* 11(2), 5600-5617. DOI: 10.15376/biores.11.2.Tajuddin

Wang, J., and Jin, H. (2019). "Research progress of wood friction welding technology," *J. Northwest For. Univ*. 34, 191-196. DOI: 10.3969/j.issn.1001-7461.2019.06.30

Yu, Z. T., Xu, X., Fan, L. W., Hu, Y. C., and Cen, K. F. (2011). "Experimental measurements of thermal conductivity of wood species in China: Effects of density, temperature, and moisture content," *Forest Products Journal* 61(2), 130-135. DOI: 10.13073/0015-7473-61.2.130

Zhang, D. H., Zhang, A. J., and Xue, L. X. (2015). "A review of preparation of binderless fiberboards and its self-bonding mechanism," *Wood Science and Technology* 49(4), 661-679. DOI: 10.1007/s00226-015-0728-6

Zhang, J.R., Gao, Y., Xu, L., Luo, X.Y. and Zhu, X.D. (2017). "Properties and mechanism of Larch with wood-dowel rotation welding," *J. Northwest For. Univ* 32, 229-234. DOI: 10.3969/j.issn.1001-7461.2017.04.38

Zhang, J., Fu, W. T., and Zhu, H. (2024). "Characterisation of rotary friction welding process and mechanism of heat-treated Scotch pine," *BioResources* 19(2), 3793-3807. DOI: 10.15376/biores.19.2.3793-3807

Zhou, X. J., Pizzi, A., and Du, G. B. (2014). "Research progress of wood welding technology (bonding without adhesive)," *China Adhesives* 23(6), 47-53. DOI: 10.13416/j.ca.2014.06.012

Zhu, H., Chen, J.R., Zhang, J., Sun, C.W. and Liu, R.F. (2020). "Influencing factors of pullout resistance on wood-dowel rotary friction welding," *Journal of Forestry Research* 48(6), 75-79. DOI: 10.3969/j.issn.1000-5382.2020.06.015

Zhu, X., Gao, Y., Yi, S., Ni, C., Zhang, J. and Luo, X. (2017). "Mechanics and pyrolysis analyses of rotation welding with pretreated wood dowels," *Journal of Wood Science* 63, 216-24. DOI: 10.1007/s10086-017-1617-4

Article submitted: March 2, 2025; Peer review completed: March 23, 2025; Revised version received: April 3, 2025; Further revised version Accepted: June 2, 2025; Published: June 18, 2025.
DOI: 10.15376/biores.20.3.6267-6285